WM-01-111
BU-01-22

U(2)-like Flavor Symmetries and Approximate Bimaximal Neutrino Mixing

Alfredo Aranda,[1,*] Christopher D. Carone,[2,†] and Patrick Meade[2,‡]

[1] *Department of Physics, Boston University, 590 Commonwealth Ave, Boston, MA 02215*

[2] *Nuclear and Particle Theory Group, Department of Physics, College of William and Mary, Williamsburg, VA 23187-8795*

(Dated: September, 2001)

Abstract

Models involving a U(2) flavor symmetry, or any of a number of its non-Abelian discrete subgroups, can explain the observed hierarchy of charged fermion masses and CKM angles. It is known that a large neutrino mixing angle connecting second and third generation fields may arise via the seesaw mechanism in these models, without a fine tuning of parameters. Here we show that it is possible to obtain approximate bimaximal mixing in a class of models with U(2)-like Yukawa textures. We find a minimal form for Dirac and Majorana neutrino mass matrices that leads to two large mixing angles, and show that our result can quantitatively explain atmospheric neutrino oscillations while accommodating the favored, large angle MSW solution to the solar neutrino problem. We demonstrate that these textures can arise in models by presenting a number of explicit examples.

*aranda@BUPHY.bu.edu
†carone@physics.wm.edu
‡prmead@mail.wm.edu

I. INTRODUCTION

New data on neutrino oscillations from experiments like SuperKamiokande [1] and SNO [2], have provided a means of testing theories of fermion masses. The simple idea that the observed hierarchies in the quark and charged lepton mass spectrum may be due to the sequential breaking of a horizontal symmetry has led to an expansive literature on possible symmetries and symmetry breaking patterns [3, 4]. Models based on non-Abelian flavor symmetries like U(2) are interesting in that Yukawa matrices decompose into a small set of flavor group representations, and the textures possible after symmetry breaking are often highly restricted. Hierarchies in these textures are not difficult to obtain, since each stage of flavor symmetry breaking is associated with a small dimensionless parameter that appears in the low-energy effective Lagrangian (namely, the ratio of a vacuum expectation value to the cut off of the effective theory). It is much harder to see how the breaking of a non-Abelian symmetry that leads to strictly hierarchical quark and charged lepton Yukawa matrices can account for the two large mixing angles suggested by the current solar and atmospheric neutrino data [6, 7]. In this paper, we will show how this situation can arise naturally in models with "U(2)-like" Yukawa textures; we define what we mean by this more explicitly below. Study of ways in which large neutrino mixing angles can arise in U(2)-like models is worthwhile since these theories can potentially explain all fermion masses and mixing angles in one consistent framework.

Let us briefly review the minimal U(2) model [5], which has been described in detail elsewhere in the literature. U(2) is assumed to be a global symmetry that acts across the three standard model generations. Quarks and leptons are assigned to $\mathbf{2} \oplus \mathbf{1}$ representations, so that in tensor notation, one may represent the three generations of any matter field by $F^a + F^3$, where a is a U(2) index, and F is Q, U, D, L, or E. A set of symmetry breaking fields are introduced consisting of ϕ_a, S_{ab} and A_{ab}, where ϕ is a U(2) doublet, and S (A) is a symmetric (antisymmetric) U(2) triplet (singlet). These fields are assumed to develop the pattern of vacuum expectation values (vevs)

$$\frac{\langle \phi \rangle}{M_f} = \begin{pmatrix} 0 \\ \epsilon \end{pmatrix}, \qquad \frac{\langle S \rangle}{M_f} = \begin{pmatrix} 0 & 0 \\ 0 & \epsilon \end{pmatrix},$$

$$\text{and} \quad \frac{\langle A \rangle}{M_f} = \begin{pmatrix} 0 & \epsilon' \\ -\epsilon' & 0 \end{pmatrix}, \tag{1.1}$$

which follows from the sequential symmetry breaking

$$U(2) \xrightarrow{\epsilon} U(1) \xrightarrow{\epsilon'} \text{nothing}. \tag{1.2}$$

This leads to the canonical U(2) texture

$$Y_D \sim \begin{pmatrix} 0 & d_1\epsilon' & 0 \\ -d_1\epsilon' & d_2\epsilon & d_3\epsilon \\ 0 & d_4\epsilon & d_5 \end{pmatrix} \xi \ , \tag{1.3}$$

where $\epsilon \approx 0.02$, $\epsilon' \approx 0.004$, and $d_1 \ldots d_5$ are order one coefficients that are also determined by fitting to the data [5]. The parameter ξ is explained below. Here we have displayed Y_D since the up quark Yukawa matrix requires additional suppression factors to explain why $m_d :: m_s :: m_b = \lambda^4 :: \lambda^2 :: 1$ while $m_u :: m_c :: m_t = \lambda^8 :: \lambda^4 :: 1$, where $\lambda \approx 0.22$ is the Cabibbo angle. For example, in SU(5)×U(2) unified models, combined GUT and flavor symmetries prevent the S and A flavons from coupling at lowest order in Y_U, provided that the S flavon is chosen to transform as a **75** under SU(5). However, the presence of an SU(5) adjoint field Σ with $\langle\Sigma\rangle/M_f \approx \epsilon$ leads to the viable texture

$$Y_U \sim \begin{pmatrix} 0 & u_1\epsilon'\epsilon & 0 \\ -u_1\epsilon'\epsilon & u_2\epsilon^2 & u_3\epsilon \\ 0 & u_4\epsilon & u_5 \end{pmatrix}. \tag{1.4}$$

The ratio m_b/m_t is fixed by hand through the choice of the small parameter ξ [5]. Note that the additional suppression factor multiplying the S and A flavon vevs can also be accommodated in models based on discrete subgroups of U(2) without requiring a grand unified embedding. In some of these models, $\xi \sim \epsilon$ is a prediction of the theory [8].

The feature crucial to the success of the U(2) model is the existence of a U(1) subgroup that rotates first generation fields by a phase. Notice that the ϵ entries in Eq (1.3) appear in the most general way consistent with this symmetry, while the ϵ' entries which break the U(1) appear only in the first row and column. The fact that the U(1) breaking is accomplished by the antisymmetric flavon A alone is a dynamical assumption, at least

at the level of the low-energy effective theory. From this point of view, there is nothing wrong with vevs of order $\epsilon' M_f$ arising, for example, in the first component of a doublet or symmetrically in the off-diagonal components of S. We will define a "U(2)-like" model as any one whose Yukawa matrices decompose into symmetric triplet, doublet, and antisymmetric singlet representations, and whose nonvanishing Yukawa entries are of a size consistent with the U(2) symmetry breaking pattern given in Eq. (1.2). Let us illustrate this definition with a concrete example:

The smallest non-Abelian discrete subgroup of U(2) with **1**, **2**, and **3** dimensional representations, and with the multiplication rule $\mathbf{2} \otimes \mathbf{2} \sim \mathbf{3} \oplus \mathbf{1}$ is the double tetrahedral group, T'. Models based on $G_f = T' \times Z_3$, and the breaking pattern [8, 9]

$$T' \times Z_3 \stackrel{\epsilon}{\to} Z_3^D \stackrel{\epsilon'}{\to} \text{nothing}, \tag{1.5}$$

can exactly reproduce the Yukawa textures of a U(2) model when matter fields are assigned to appropriate one- and two-dimensional representations. The symmetry Z_3^D is a diagonal subgroup that provides the desired phase rotation on first generation fields. Moreover, doublet, triplet and nontrivial singlet T' representations can be found that are in one-to-one correspondence with the ϕ, S, and A flavons of the original U(2) model. In Ref [8], models based on T' symmetry were constructed with an additional doublet flavon that affected only the neutrino mass matrix textures:

$$\frac{\langle \phi_\nu \rangle}{M_f} \sim \begin{pmatrix} \epsilon' \\ \epsilon \end{pmatrix}. \tag{1.6}$$

The pattern of vevs in ϕ_ν is the most general one consistent with Eq. (1.5) and leads to the neutrino mass matrix textures [8]

$$M_{LR} = \begin{pmatrix} 0 & l_1\epsilon' & l_3\epsilon' \\ -l_1\epsilon' & l_2\epsilon & l_3\epsilon \\ 0 & l_4\epsilon & 0 \end{pmatrix} \langle H_U \rangle \ , \tag{1.7}$$

$$M_{RR} = \begin{pmatrix} r_4\epsilon'^2 & r_4\epsilon\epsilon' & \epsilon' \\ r_4\epsilon\epsilon' & r_3\epsilon & \epsilon \\ \epsilon' & \epsilon & 0 \end{pmatrix} \Lambda_R \ , \tag{1.8}$$

where Λ_R is the right-handed neutrino mass scale, and r_i, l_i are $O(1)$ coefficients. These textures are U(2)-like in that each entry is of a size consistent with the two-stage symmetry breaking pattern in Eq. (1.2); the precise power of ϵ or ϵ' that appears is determined in this example by the details of the T' group theory. The left-handed Majorana mass matrix follows from the seesaw mechanism

$$M_{LL} \approx M_{LR} M_{RR}^{-1} M_{LR}^{\dagger} \tag{1.9}$$

and has the form

$$M_{LL} \sim \begin{pmatrix} (\epsilon'/\epsilon)^2 & \epsilon'/\epsilon & \epsilon'/\epsilon \\ \epsilon'/\epsilon & 1 & 1 \\ \epsilon'/\epsilon & 1 & 1 \end{pmatrix} \frac{\langle H_U \rangle^2 \epsilon}{\Lambda_R} \tag{1.10}$$

As promised, a large 2-3 mixing angle has emerged from initial U(2)-like textures without any adjustment of parameters. The 1-2 mixing angle, of order ϵ'/ϵ, is naturally of the same size as the Cabibbo angle. By choosing the $O(1)$ coefficients appropriately, it is possible to numerically enhance this result to obtain the smallest mixing angle values consistent with the MSW large mixing angle (LMA) allowed parameter region given in Ref. [6]. Such solutions were considered in quantitative detail in Ref. [10]. However, the fact that the current data appears to prefer relatively large mixing angles suggests another possibility: M_{LL} is a perturbation about a bimaximal mixing texture [11] that appears at lowest order in the symmetry breaking parameters. It is this possibility that we explore in the sections that follow.

II. APPROXIMATE BIMAXIMAL MIXING

What is intriguing about the result in Eq. (1.10) is that it is superficially of the form suggested by Haba [12] for achieving bimaximal mixing,

$$M_{LL} \sim \begin{pmatrix} \Phi^2 & \Phi & \Phi \\ \Phi & 1 & 1 \\ \Phi & 1 & 1 \end{pmatrix} M_0 \ , \tag{2.1}$$

where Φ is a small parameter, and M_0 a characteristic mass scale. The crucial difference is that the $O(1)$ sub-block of the Haba texture is assumed to be of rank one, up to corrections

of order Φ or smaller. A diagonalization of the largest entries leaves a matrix of the form

$$M_{LL} \sim \begin{pmatrix} \Phi^2 & \Phi & \Phi \\ \Phi & \Phi & 0 \\ \Phi & 0 & 1 \end{pmatrix} M_0 \ , \tag{2.2}$$

which requires a large 1-2 rotation angle to diagonalize further. We now demonstrate that it is possible to achieve the Haba texture via the seesaw mechanism in U(2)-like theories.

Our approach is to determine first the minimal number of entries in M_{LR} and M_{RR} that can reproduce the rank-one sub-block of Eq. (2.1). We will then perturb about this texture by lifting the smallest number of texture zeros that allows for a viable phenomenology. The only organizing principle that we retain in this model-independent analysis is that entries in the first row and column of M_{LR} and M_{RR} must involve the appropriate power of ϵ' to be consistent with the breaking of some subgroup that rotates the fields of the first generation by a phase.

We begin with the observation that the matrices

$$M_{LR} = \begin{pmatrix} 0 & 0 & 0 \\ -l_1\epsilon' & 0 & 0 \\ 0 & l_3\epsilon & 0 \end{pmatrix} \langle H_U \rangle \tag{2.3}$$

and

$$M_{RR} = \begin{pmatrix} 0 & 0 & r_2\epsilon' \\ 0 & r_1\epsilon & r_2\epsilon \\ r_2\epsilon' & r_2\epsilon & 0 \end{pmatrix} \Lambda_R \tag{2.4}$$

lead via the seesaw to

$$M_{LL} = \frac{\epsilon}{r_1} \begin{pmatrix} 0 & 0 & 0 \\ 0 & l_1^2 & l_1 l_3 \\ 0 & l_1 l_3 & l_3^2 \end{pmatrix} \frac{\langle H_U \rangle^2}{\Lambda_R} \ . \tag{2.5}$$

The sub-block has a vanishing determinant, by inspection[1]. It is clear from Eq. (2.5) that the entries shown in (2.3) and (2.4) are a minimal choice; if one sets any of the parameters to zero, one either renders M_{RR} singular or loses the large 2-3 mixing angle in the final

[1] Note that the parameterization in Eqs. (2.3) and (2.4) is completely general, given that we have not specified the size of ϵ or ϵ'.

result. Note also that the textures in Eqs. (2.3) and (2.4) are consistent with the symmetry breaking in Eq (1.2), but require one fine tuning to be obtained: The 1-2 block of M_{LR} can arise only by a specific linear combination of symmetric and antisymmetric flavon vevs. In the more realistic textures that follow, such a fine tuning will not be required. Finally, we point out that certain texture zeros, in particular the 3-3 entries of M_{LR} and M_{RR}, do not appear in the simplest formulation of U(2) models. However, as we mentioned earlier, such textures do arise in models based on discrete subgroups of U(2) [8, 9]. In Section 4 we will see how they can also arise in models with U(2) symmetry and additional Abelian factors.

We now seek the minimal modifications of Eqs. (2.3) and (2.4) that provide for a viable phenomenology and are theoretically well motivated. To avoid any fine tuning between irreducible symmetric and antisymmetric representations, the first zero that we choose to lift is the 1-2 entry of M_{LR}. Hence, we consider the modification

$$M'_{LR} = \begin{pmatrix} 0 & l_1\epsilon' & 0 \\ -l_1\epsilon' & 0 & 0 \\ 0 & l_3\epsilon & 0 \end{pmatrix} \langle H_U \rangle \tag{2.6}$$

which leads to

$$M'_{LL} = \frac{\epsilon}{r_1} \begin{pmatrix} l_1^2(\epsilon'/\epsilon)^2 & l_1^2(\epsilon'/\epsilon) & l_1 l_3(\epsilon'/\epsilon) \\ l_1^2(\epsilon'/\epsilon) & l_1^2 & l_1 l_3 \\ l_1 l_3(\epsilon'/\epsilon) & l_1 l_3 & l_3^2 \end{pmatrix} \frac{\langle H_U \rangle^2}{\Lambda_R}. \tag{2.7}$$

If we identify ϵ'/ϵ with Φ, we obtain a texture of the same form as Eq. (2.1), with the desired rank one sub-block. Unfortunately, the texture in Eq. (2.7) is still not viable due to a specific relationship between the coefficients: the 1-2 and 1-3 entries appear in the same ratio as the 2-2 and 2-3 entries. Diagonalization of the largest elements leaves a matrix of the form

$$M_{LL} \sim \begin{pmatrix} \Phi^2 & 0 & \Phi \\ 0 & 0 & 0 \\ \Phi & 0 & 1 \end{pmatrix} M_0 \tag{2.8}$$

and no large 1-2 mixing angle is obtained. It is necessary to lift at least one additional texture zero in order to disrupt this proportionality of coefficients. We find that the minimal choice,

in which only one additional entry is altered, is unique:

$$M_{RR} = \begin{pmatrix} 0 & 0 & r_2\epsilon' \\ 0 & r_1\epsilon & r_2\epsilon \\ r_2\epsilon' & r_2\epsilon & 0 \end{pmatrix} \Lambda_R, \qquad M''_{LR} = \begin{pmatrix} 0 & l_1\epsilon' & l_2\epsilon' \\ -l_1\epsilon' & 0 & 0 \\ 0 & l_3\epsilon & 0 \end{pmatrix} \langle H_U \rangle \ . \tag{2.9}$$

From here we finally obtain

$$M''_{LL} = \frac{\epsilon}{r_1} \begin{pmatrix} l_1^2(\epsilon'/\epsilon)^2 & (l_1^2 - l_1 l_2 r_1/r_2)(\epsilon'/\epsilon) & l_1 l_3(\epsilon'/\epsilon) \\ (l_1^2 - l_1 l_2 r_1/r_2)(\epsilon'/\epsilon) & l_1^2 & l_1 l_3 \\ l_1 l_3(\epsilon'/\epsilon) & l_1 l_3 & l_3^2 \end{pmatrix} \frac{\langle H_U \rangle^2}{\Lambda_R} \ . \tag{2.10}$$

We will refer to Eqs. (2.9) and (2.10) as our minimal bimaximal mixing textures.

At this point, it is important that we be specific on the meaning of the zero entries in Eq. (2.10). We assume simply that there are no contributions to these entries at linear order in the symmetry-breaking parameters. As we will see in Section 4, most realistic models imply that texture zeroes are lifted at some order in the flavor expansion, unless those entries are protected by holomorphy. This is of significance to the phenomenological analysis presented in the next section for the following reason: While the ratio $\Delta m^2_{23}/\Delta m^2_{12} \approx \epsilon^2/\epsilon'^2 \approx 25$ that follows from Eq. (2.10) is naturally of the right size to account for atmospheric and LMA solar neutrino oscillations, the experimentally preferred value of θ_{12} is noticeably less than 45°. Corrections to the zero entries allow us numerically to obtain mixing angles consistent with allowed 95% confidence region. In particular, we will study the more general form

$$M_{RR} = \begin{pmatrix} 0 & 0 & r_2\epsilon' \\ 0 & r_1\epsilon & r_2\epsilon \\ r_2\epsilon' & r_2\epsilon & r_3\epsilon^2 \end{pmatrix} \Lambda_R, \qquad M''_{LR} = \begin{pmatrix} 0 & l_1\epsilon' & l_2\epsilon' \\ -l_1\epsilon' & 0 & 0 \\ 0 & l_3\epsilon & 0 \end{pmatrix} \langle H_U \rangle \ . \tag{2.11}$$

since the higher-order r_3 entry is quite effective at allowing adjustment of θ_{12}, and is easily accommodated in realistic models. It is worth pointing out that U(2)-like values for ϵ and ϵ' are not consistent with the LOW or vacuum oscillation solutions to the solar neutrino problem, since each requires a value of $\Delta m^2_{23}/\Delta m^2_{12}$ that is much larger than that predicted from Eq. (2.10).

III. NUMERICAL ANALYSIS

We now study the textures in Eq. (2.9) and (2.11) numerically, and show that atmospheric and large angle solar neutrino oscillations can be obtained. In the spirit of model independence, we assume a form for the charged lepton Yukawa matrix that arises generically in U(2)-like models:

$$Y_L \sim \begin{pmatrix} 0 & c_1\epsilon' & 0 \\ -c_1\epsilon' & 3c_2\epsilon & c_3\epsilon \\ 0 & c_4\epsilon & c_5 \end{pmatrix} \xi \ . \tag{3.1}$$

The factor of 3 that multiplies c_2 is the famous one suggested by Georgi and Jarlskog [13], and arises as a consequence of grand unified group theory. We fit to leptonic observables while fixing $\epsilon = 0.02$ and $\epsilon' = 0.004$; these are the preferred values obtained in fitting Eq. (1.3) and Eq. (1.4) to quark masses and CKM angles. This constrained fit is a reasonable approximation to a more involved global one, given the relatively large experimental uncertainty on each of the neutrino observables.

We assume that the textures M_{LL} and Y_L are defined at some high scale, which we take to be $M_{\rm GUT} \approx 2 \times 10^{16}$ GeV, and perform a renormalization group analysis of the gauge and Yukawa couplings. We do this by solving the one-loop renormalization group equations (RGE's) of the MSSM [14] from $M_{\rm GUT}$ down to the electroweak scale taken to be $m_t = 175$ GeV.

Values of the gauge couplings at $M_{\rm GUT}$ are obtained by starting with the precision values extracted at the scale M_Z [15],

$$\begin{aligned} \alpha_1^{-1}(M_Z) &= 59.99 \pm 0.04, \\ \alpha_2^{-1}(M_Z) &= 29.57 \pm 0.03, \\ \alpha_3^{-1}(M_Z) &= 8.40 \pm 0.13. \end{aligned} \tag{3.2}$$

The gauge couplings are run from M_Z to m_t using the one-loop Standard Model (SM) RGE's, and then from m_t to $M_{\rm GUT}$ using the one-loop MSSM RGE's. The RGE for the neutrino Majorana mass matrix M_{LL} was computed in Ref. [16] and is included here in order to complete the RGE evolution for all observables.

In order to perform the fits we incorporate experimental and theoretical uncertainties on the observables. For the charged leptons, they are either those appearing in Ref. [15]

or 1% of the central value of the given datum, whichever is larger. The latter, theoretical uncertainty takes into account that two-loop corrections to the running and possible high-scale threshold corrections have been neglected. The low-energy neutrino observables are taken to be

$$\begin{aligned} & 4 < \frac{\Delta m^2_{23}}{\Delta m^2_{12}} < 200, \\ & \sin^2 2\theta_{23} > 0.88, \\ & 0.2 < \tan^2\theta_{12} < 0.9 \ , \end{aligned} \tag{3.3}$$

which were extracted from Refs. [6, 17]. Notice that we only need to reproduce the ratio $\Delta m^2_{23}/\Delta m^2_{12}$ since the right-handed neutrino scale Λ_R is freely adjustable. For the sake of having meaningful uncertainties, a parameter whose lower bound is much smaller than its upper bound is converted into its logarithm. Instead of Eq. (3.3), we use

$$\begin{aligned} \ln\left(\frac{\Delta m^2_{23}}{\Delta m^2_{12}}\right) &= 3.34 \pm 0.98, \\ \sin^2 2\theta_{23} &= 0.94 \pm 0.03, \\ \tan^2\theta_{12} &= 0.55 \pm 0.18. \end{aligned} \tag{3.4}$$

In order to determine whether one can find a choice of parameters (generically denoted by k_i) which are $O(1)$ and at the same time reproduce the values of observables, we perform a χ^2 minimization. The full analysis consists of choosing initial values for the $O(1)$ coefficients k_i, for fixed[2] $\tan\beta$, running the RGE's down to m_t, and comparing observables with their experimental values to compute χ^2. Then, the parameters k_i are adjusted and the procedure repeated until a minimum of χ^2 is obtained.

Our χ^2 function assumes a somewhat nonstandard form. Lepton masses and neutrino mixing angles are converted to Yukawa couplings $y_i^{\rm expt} \pm \Delta y_i$, and contribute an amount

$$\Delta\chi^2 = \left(\frac{y_i^{\rm expt} - y_i}{\Delta y_i}\right)^2 \tag{3.5}$$

to χ^2, as usual. There are 6 observables (3 charged lepton masses, 2 neutrino mixing angles, and 1 neutrino mass ratio) and 11 parameters k_i; on the surface, it seems that the fit

[2] We work with $\tan\beta = 3$. Qualitatively, our results are insensitive to changes in $\tan\beta$ of order unity.

Observable	Expt. value	Fit A	Fit B	Fit C	Fit D
m_e	$0.511 \pm 1\%$	0.512	0.511	0.511	0.512
m_μ	$106 \pm 1\%$	106	106	106	106
m_τ	$1777 \pm 1\%$	1778	1777	1778	1777
$\Delta m^2_{23}/\Delta m^2_{12}$	4—200	40	34	35	42
$\ln(\Delta m^2_{23}/\Delta m^2_{12})$	3.34 ± 0.98	3.7	3.5	3.6	3.7
$\tan^2\theta_{12}$	0.20 — 0.90	0.89	0.66	0.66	0.88
$\sin^2 2\theta_{23}$	> 0.88	0.94	0.93	0.94	0.93
$\sin^2 2\theta_{13}$	< 0.1—0.3	0.24	0.01	0.04	0.24

TABLE I: Experimental values versus fit central values for observables using the inputs of Table II. Masses are in MeV and all other quantities are dimensionless. Error ranges indicate the larger of experimental or 1% theoretical uncertainties, as described in the text.

is always under-constrained. However, our demand that the parameters k_i lie near unity imposes additional restrictions, which we include by adding terms to χ^2 of the form

$$\Delta\chi^2 = \left(\frac{\ln|k_i|}{\ln 3}\right)^2 \tag{3.6}$$

for each i. Thus, the parameters k_i are effectively no longer free, but are to be treated analogously to pieces of data, each of which contributes one unit to χ^2 if it is as large as 3 or as small as $1/3$ [3]. Thus, the value of $\chi^2_{\rm min}$ determining a 'good' fit is 6, since there are 6 pieces of true data and effectively no *unconstrained* fit parameters. We find that it is not difficult to obtain parameters k_i that work, as one can see in Tables I and II.

For each fit shown a value of the mixing angle θ_{13} was obtained. While there is no experimental evidence for 1-3 neutrino oscillations, an eventual positive signal could help to distinguish between possible models. In Fig. 1, we plot the values of θ_{13} vs. χ^2 for a number of different fits. Each dot in the figure corresponds to a different set of randomly generated initial values for the parameters k_i, *i.e.* a different local minimum of the χ^2 function. We compare this to the bound $\sin^2 2\theta_{13} < 0.1 - 0.3$ [18], which is indicated in the figure by horizontal lines. The green dots correspond to fits where θ_{12} is above the 95% C.L. bound.

[3] The choice of 3 is a matter of taste.

Fit	A	B	C	D
χ^2	3.451421	2.98341084	3.72175717	8.29507256
c_1	0.47674	0.476627409	0.476760209	0.476436228
c_2	0.46998	−0.465719551	−0.440337121	0.462245226
c_3	0.99173	0.82251513	1.39617729	0.9901492
c_4	1.0226	0.89786166	0.76331389	0.559998155
c_5	0.45998	−0.460312963	0.46006763	0.460330635
l_1	1.3715	1.1396178	0.674030304	0.434771806
l_2	−0.51276	1.21720707	1.68183231	1.90096331
l_3	1.4191	1.14355946	0.920410395	0.600989103
r_1	1.1785	1.16333687	1.38230038	0.481762707
r_2	0.36925	0.381390542	0.589898586	0.280204356
r_3	2.2979	−1.69190395	−2.8438561	0.0

TABLE II: O(1) coefficients from four representative fits with $\tan\beta = 3.0$. The observables computed using these values are shown in Table I. Fit D correspond to the minimal $r_3 = 0$ case.

IV. MODELS

We now demonstrate that it is possible to construct models that realize the textures studied numerically in the previous section. We aim for the basic forms

$$M_{RR} = \begin{pmatrix} 0 & 0 & r_2\epsilon' \\ 0 & r_1\epsilon & r_2\epsilon \\ r_2\epsilon' & r_2\epsilon & 0 \end{pmatrix} \Lambda_R, \qquad M''_{LR} = \begin{pmatrix} 0 & l_1\epsilon' & l_2\epsilon' \\ -l_1\epsilon' & 0 & 0 \\ 0 & l_3\epsilon & 0 \end{pmatrix} \langle H_U \rangle \ . \tag{4.1}$$

As mentioned earlier, it will require more than just U(2) symmetry to account for these textures. For one, there is no invariant 3-3 entry in each matrix, as one would expect in a minimal U(2) model with the generations assigned to $\mathbf{2}+\mathbf{1}$ representations. Moreover, these textures imply the existence of three doublet fields, with distinct couplings, while U(2) provides only for one. The simplest approach, which we will utilize here for the purposes of providing an existence proof, is to extend the U(2) symmetry by an additional Abelian factor [19]. At the end, we describe how similar models may be obtained using non-Abelian

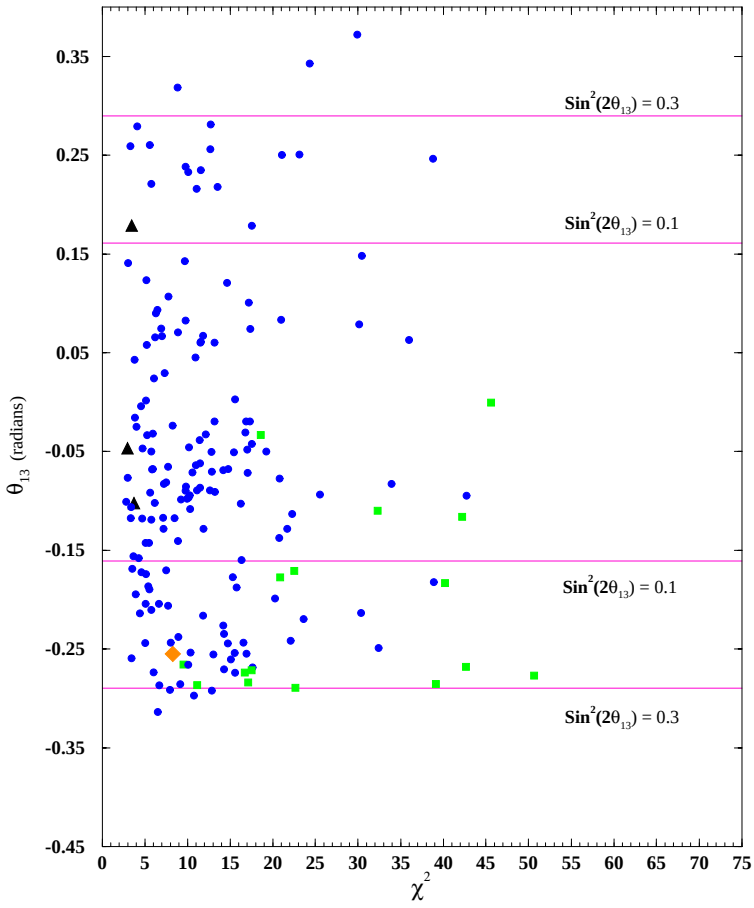

FIG. 1: Values of θ_{13} vs. χ^2 for 202 different randomly generated fits. The horizontal lines are the bounds discussed in the text. Blue dots correspond to fits in which all observables are within the desired experimental 95% C.L. regions for atmospheric and LMA solar neutrino oscillations. Green squares correspond to fits that had a θ_{12} slightly above the upper bound for the LMA solution. The 3 black triangles correspond to the fits A, B, and C, and the orange diamond is the best fit with $r_3 = 0$, i.e. fit D in the text.

discrete subgroups of U(2). We present examples that do and do not require a unified gauge group, respectively:

A. $\mathbf{SU(5)\times U(2)\times}Z_5$

In this model we let the superfields Q, U, D, L, E transform as

$$\mathbf{2}_0 \oplus \mathbf{1}_0 \tag{4.2}$$

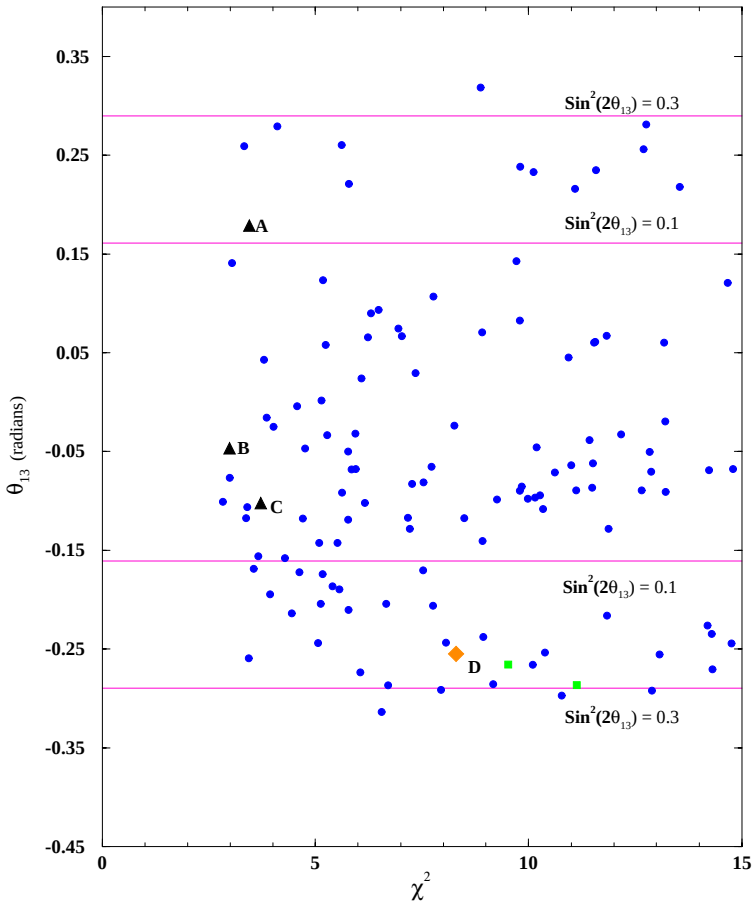

FIG. 2: Here we show the fits with a $\chi^2 < 15$.

where the subscript indicates the Z_5 charge (*i.e.* the subscripts add modulo 5). The Higgs fields $H_{U,D}$ transform as trivial singlets under both $U(2)$ and Z_5. In addition, there is a set of 'ordinary' flavons that are Z_5 singlets, but transform under SU(5) as follows:

$$\begin{aligned} S_0 &\sim 3_0 \sim \mathbf{75} \\ A_0 &\sim 1_0 \sim \mathbf{1} \\ \phi_0 &\sim 2_0 \sim \mathbf{1} \end{aligned} \tag{4.3}$$

These assignments allow us to reproduce the conventional Yukawa textures of the unified SU(5)×U(2) model. The desired neutrino textures are obtained by introducing right-handed neutrinos transforming non-trivially under the Z_5 factor:

$$\nu_R \sim \mathbf{2}_2 \oplus \mathbf{1}_4 \tag{4.4}$$

The neutrino Dirac and Majorana mass matrices decompose under this symmetry as

$$M_{LR} \sim \begin{pmatrix} [\mathbf{3_3} \oplus \mathbf{1_3}] & [\mathbf{2_1}] \\ [\mathbf{2_3}] & [\mathbf{1_1}] \end{pmatrix}, \qquad M_{RR} \sim \begin{pmatrix} [\mathbf{3_1}] & [\mathbf{2_4}] \\ [\mathbf{2_4}] & [\mathbf{1_2}] \end{pmatrix} \ . \tag{4.5}$$

We introduce the SU(5)-singlet flavons

$$\frac{\langle A_3 \rangle}{M_f} \sim \mathbf{1_3} \sim \begin{pmatrix} 0 & \epsilon' \\ -\epsilon' & 0 \end{pmatrix}, \qquad \frac{\langle S_1 \rangle}{M_f} \sim \mathbf{3_1} \sim \begin{pmatrix} 0 & 0 \\ 0 & \epsilon \end{pmatrix},$$

$$\frac{\langle \phi_3 \rangle}{M_f} \sim \mathbf{2_3} \sim \begin{pmatrix} 0 \\ \epsilon \end{pmatrix}, \qquad \frac{\langle \phi_1 \rangle}{M_f} \sim \mathbf{2_1} \sim \begin{pmatrix} \epsilon' \\ 0 \end{pmatrix}, \qquad \frac{\langle \phi_4 \rangle}{M_f} \sim \mathbf{2_4} \sim \begin{pmatrix} \epsilon' \\ \epsilon \end{pmatrix} \ , \tag{4.6}$$

and thus arrive at the correct textures for M_{LR} and M_{RR}:

$$M_{LR} \sim \begin{pmatrix} A_3 & \phi_1 \\ \phi_3 & 0 \end{pmatrix} \sim \begin{pmatrix} 0 & \epsilon' & \epsilon' \\ -\epsilon' & 0 & 0 \\ 0 & \epsilon & 0 \end{pmatrix} \langle H_U \rangle \ , \tag{4.7}$$

$$M_{RR} \sim \begin{pmatrix} S_1 & \phi_4 \\ \phi_4 & 0 \end{pmatrix} \sim \begin{pmatrix} 0 & 0 & \epsilon' \\ 0 & \epsilon & \epsilon \\ \epsilon' & \epsilon & 0 \end{pmatrix} \Lambda_R \ . \tag{4.8}$$

Notice that the Z_5 charge assignments of the new flavons prevent them from affecting the lowest order textures for Y_U, Y_D and Y_E. Thus, the predictions of the minimal unified U(2) model are maintained. The pattern of vevs in the doublet flavons is a dynamical assumption, at the level of our effective field theory analysis, but is at least well motivated: it is known that minima of potentials occur at enhanced symmetry points, and the pattern of vevs is one consistent with the sequential breaking in Eq. (1.2). Presumably, an explicit high-energy model would involve a complicated flavon potential, and different patterns of ϵ and ϵ' might arise depending on differing parameter choices. We do not consider this issue further in this paper. For some discussion of possible flavon potentials in U(2) models, see Ref. [20]. Finally, we point out that the presence of additional fields with vacuum expectation values can perturb these textures; this is not unlikely given that additional fields are usually required in constructing a realistic flavon potential. As an example, the presence of a doublet $\overline{\phi}_4$ transforming as $\overline{\mathbf{2}}_\mathbf{4}$ with an ϵ vev alters none of these textures at lowest order. (Unlike SU(2), the $\mathbf{2}$ and $\overline{\mathbf{2}}$ reps are distinct.) However, the product $\overline{\phi}_4 \phi_3 \sim \mathbf{1_2}$ provides the ϵ^2 perturbation in the 3-3 entry of M_{RR} considered in the numerical analysis.

B. U(2)×U(1)

Here we show that the inclusion of an additional U(1) symmetry is sufficient for constructing viable models, even if there is no unified gauge group. Aside from predicting our desired textures Eq. (4.1), we now must also account for the additional suppression factor in Y_U, discussed in the Introduction, that originated previously from the SU(5) transformation properties of the flavons. We accomplish this by allowing the charged fermions to transform nontrivially under the additional symmetry. We let

$$\begin{aligned} Q, U, E &\sim \mathbf{2}_1 \oplus \mathbf{1}_0 \\ D, L &\sim \mathbf{2}_1 \oplus \mathbf{1}_1 \end{aligned} \tag{4.9}$$

while the Higgs fields and the right-handed neutrinos transform as

$$\begin{aligned} H_{U,D} &\sim \mathbf{1}_0 \\ \nu_R &\sim \mathbf{2}_0 \oplus \mathbf{1}_3 \end{aligned} \tag{4.10}$$

Proceeding as before, the various Yukawa and mass matrices have the transformation properties:

$$Y_U \sim \begin{pmatrix} [\mathbf{3_{-2}} \oplus \mathbf{1_{-2}}] & [\mathbf{2_{-1}}] \\ [\mathbf{2_{-1}}] & [\mathbf{1_0}] \end{pmatrix} \quad Y_D \sim \begin{pmatrix} [\mathbf{3_{-2}} \oplus \mathbf{1_{-2}}] & [\mathbf{2_{-2}}] \\ [\mathbf{2_{-1}}] & [\mathbf{1_{-1}}] \end{pmatrix} \quad Y_L \sim \begin{pmatrix} [\mathbf{3_{-2}} \oplus \mathbf{1_{-2}}] & [\mathbf{2_{-1}}] \\ [\mathbf{2_{-2}}] & [\mathbf{1_{-1}}] \end{pmatrix}$$

$$M_{LR} \sim \begin{pmatrix} [\mathbf{3_{-1}} \oplus \mathbf{1_{-1}}] & [\mathbf{2_{-4}}] \\ [\mathbf{2_{-1}}] & [\mathbf{1_{-4}}] \end{pmatrix} \qquad M_{RR} \sim \begin{pmatrix} [\mathbf{3_0}] & [\mathbf{2_{-3}}] \\ [\mathbf{2_{-3}}] & [\mathbf{1_{-6}}] \end{pmatrix} \tag{4.11}$$

We introduce the set of flavons

$$\frac{\langle S_0 \rangle}{M_f} \sim 3_0 \sim \begin{pmatrix} 0 & 0 \\ 0 & \epsilon \end{pmatrix} \qquad \frac{\langle A_{-1} \rangle}{M_f} \sim 1_{-1} \sim \begin{pmatrix} 0 & \epsilon' \\ -\epsilon' & 0 \end{pmatrix}$$

$$\frac{\langle \phi_{-1} \rangle}{M_f} \sim 2_{-1} \sim \begin{pmatrix} 0 \\ \epsilon \end{pmatrix} \qquad \frac{\langle \phi_{-3} \rangle}{M_f} \sim 2_{-3} \sim \begin{pmatrix} \epsilon' \\ \epsilon \end{pmatrix} \qquad \frac{\langle \phi_{-4} \rangle}{M_f} \sim 2_{-4} \sim \begin{pmatrix} \epsilon' \\ 0 \end{pmatrix}$$

$$\frac{\langle \chi_{-1} \rangle}{M_f} \sim 1_{-1} \sim \epsilon \tag{4.12}$$

from which we obtain

$$Y_U \sim \begin{pmatrix} \phi^2_{-1} + A_{-1}\chi_{-1} & \phi_{-1} \\ \phi_{-1} & 1 \end{pmatrix} \sim \begin{pmatrix} 0 & \epsilon\epsilon' & 0 \\ -\epsilon\epsilon' & \epsilon^2 & \epsilon \\ 0 & \epsilon & 1 \end{pmatrix} \tag{4.13}$$

$$Y_D \sim \begin{pmatrix} \phi_{-1}^2 + A_{-1}\chi_{-1} & \phi_{-1}\chi_{-1} \\ \phi_{-1} & \chi_{-1} \end{pmatrix} \sim \begin{pmatrix} 0 & \epsilon' & 0 \\ -\epsilon' & \epsilon & \epsilon \\ 0 & 1 & 1 \end{pmatrix} \epsilon \tag{4.14}$$

$$Y_L \sim \begin{pmatrix} \phi_{-1}^2 + A_{-1}\chi_{-1} & \phi_{-1} \\ \phi_{-1}\chi_{-1} & \chi_{-1} \end{pmatrix} \sim \begin{pmatrix} 0 & \epsilon' & 0 \\ -\epsilon' & \epsilon & 1 \\ 0 & \epsilon & 1 \end{pmatrix} \epsilon \ , \tag{4.15}$$

as well as the neutrino Dirac and Majorana mass matrices

$$M_{LR} \sim \begin{pmatrix} A_{-1} & \phi_{-4} \\ \phi_{-1} & 0 \end{pmatrix} \sim \begin{pmatrix} 0 & \epsilon' & \epsilon' \\ -\epsilon' & 0 & 0 \\ 0 & \epsilon & 0 \end{pmatrix} \langle H_U \rangle \tag{4.16}$$

$$M_{RR} \sim \begin{pmatrix} S_0 & \phi_{-3} \\ \phi_{-3} & 0 \end{pmatrix} \sim \begin{pmatrix} 0 & 0 & \epsilon' \\ 0 & \epsilon & \epsilon \\ \epsilon' & \epsilon & 0 \end{pmatrix} \Lambda_R \tag{4.17}$$

The U(1) charges in this model allow us to obtain the desired suppression factors in Y_U, without necessitating nontrivial GUT transformation properties for the flavons, assuming a GUT is present at all. While Eqs. (4.16) and (4.17) are of the desired form for neutrino phenomenology, it should be noted that this particular model also provides for a large 2-3 mixing angle via the diagonalization of Y_L. The numerical analysis for these textures would therefore be slightly different from that presented in Section 3, but the results would be qualitatively unchanged.

C. Discrete Subgroups

Finally, we mention briefly that any of the models we have discussed (and in fact any U(2) model described in the literature [21]) can be mapped to an equivalent model based on the discrete group T'. For example, one possible mapping is

$$\mathbf{3} \to \mathbf{3} \quad \mathbf{2} \to \mathbf{2^-} \quad \mathbf{1} \to \mathbf{1^0} \ ,$$

where the notation for T' representations shown on the right is explained in Refs. [8, 9]. Other mappings exist that render a given model free of discrete gauge anomalies [22], at

least if the anomalies associated with Abelian factors are canceled via the Green-Schwarz mechanism [23]. Thus, realizations of the textures we have studied in models with discrete gauge flavor symmetries are also possible. (For other approaches to reproducing U(2) physics from discrete groups, see Ref. [24].)

V. CONCLUSIONS

In this paper, we have illustrated a simple point: Models based on spontaneously broken non-Abelian symmetries can naturally provide for two large neutrino mixing angles, even while quark and charged lepton Yukawa textures are hierarchical. In particular, we have considered U(2)-like textures – textures that can arise in a variety of models that incorporate the two-step breaking of a non-Abelian symmetry with a subgroup that rotates first generation fields by a phase. We showed how bimaximal mixing could be obtained in such models without tuning of parameters, and how perturbations about these textures, arising in realistic models, could quantitatively explain atmospheric and large-angle solar neutrino oscillations. Finally, we presented a number of toy models that reproduce the textures that we considered numerically in our model-independent discussion. While these models are viable, they nonetheless suggest that better high-energy realizations are yet to be found. The ideas presented here may therefore be useful in the eventual formulation of a compelling and comprehensive theory of fermion masses.

Acknowledgments

C.D.C. and P.M. thank the National Science Foundation for support under Grant No. PHY-9900657, and the Jeffress Memorial Trust for support under Grant No. J-532. A.A.'s work was supported in part by the Department of Energy under grant DE-FG02-91ER40676.

---

[1] See for example, Y. Oyama [SuperKamiokande collaboration], hep-ex/0104015.

[2] Q. R. Ahmad *et al.* [SNO Collaboration], Phys. Rev. Lett. **87**, 071301 (2001) [nucl-ex/0106015].

[3] Y. Nir and N. Seiberg, Phys. Lett. B **309**, 337 (1993); M. Leurer, Y. Nir, and N. Seiberg, Nucl. Phys. **B420**, 468; L.E. Ibáñez and G.G. Ross, Phys. Lett. B **332**, 100 (1994); P. Binetruy and P. Ramond, *ibid.* **350**, 49 (1995); V. Jain and R. Shrock, *ibid.* **352**, 83 (1995); Stony Brook Report No. ITP-SB-95-22, hep-ph/9507238 (unpublished); Y. Nir, Phys. Lett. B **354**, 107 (1995); E. Dudas, S. Pokorski, and C.A. Savoy, *ibid.* **356**, 45 (1995); M.M. Robinson and J. Ziabicki, Phys. Rev. D **53**, 5924 (1996); E. Dudas, S. Pokorski, and C.A. Savoy, Phys. Lett. B **369**, 255 (1996); A. Pomarol and D. Tommasini, Nucl. Phys. **B466**, 3 (1996).

[4] D.B. Kaplan and M. Schmaltz, Phys. Rev. D **49**, 3741 (1994); M. Dine, R. Leigh, and A. Kagan, Phys. Rev. D **48**, 4269 (1993); L.J. Hall and H. Murayama, Phys. Rev. Lett. **75**, 3985 (1995); C.D. Carone, L.J. Hall, and H. Murayama, Phys. Rev. D **53**, 6282 (1996); P.H. Frampton and O.C.W. Kong, Phys. Rev. Lett. **77**, 1699 (1996); C. D. Carone and R. F. Lebed, Phys. Rev. D **60**, 096002 (1999)

[5] R. Barbieri, G. Dvali, and L.J. Hall, Phys. Lett. B **377**, 76 (1996); R. Barbieri, L.J. Hall, and A. Romanino, Phys. Lett. B **401**, 47; (1997); R. Barbieri, L.J. Hall, S. Raby and A. Romanino, Nucl. Phys. **B493**, 3 (1997). C.D. Carone and L.J. Hall, Phys. Rev. D **56**, 4198 (1997); R. Barbieri, P. Creminelli and A. Romanino, Nucl. Phys. B **559** (1999) 17.

[6] J. N. Bahcall, M. C. Gonzalez-Garcia and C. Pena-Garay, JHEP **0108**, 014 (2001) [hep-ph/0106258].

[7] V. Barger, D. Marfatia and K. Whisnant, hep-ph/0106207.

[8] A. Aranda, C. D. Carone and R. F. Lebed, Phys. Lett. B **474**, 170 (2000) [hep-ph/9910392].

[9] A. Aranda, C. D. Carone and R. F. Lebed, Phys. Rev. D **62**, 016009 (2000) [hep-ph/0002044].

[10] A. Aranda, C. D. Carone and R. F. Lebed, hep-ph/0010144.

[11] V. Barger, S. Pakvasa, T. J. Weiler and K. Whisnant, Phys. Lett. B **437**, 107 (1998); H. Georgi and S. L. Glashow, Phys. Rev. D **61**, 097301 (2000); R. N. Mohapatra, hep-ph/0107264; M. Jezabek, Nucl. Phys. Proc. Suppl. **100**, 276 (2001); K. Choi, E. J. Chun, K. Hwang and W. Y. Song, hep-ph/0107083; W. Krolikowski, hep-ph/0102016; S. K. Kang and C. S. Kim, Phys. Rev. D **59**, 091302 (1999); Q. Shafi and Z. Tavartkiladze, hep-ph/0101350; W. Krolikowski, Acta Phys. Polon. B **32**, 1245 (2001); Y. Koide and A. Ghosal, Phys. Rev. D **63**, 037301 (2001); D. V. Ahluwalia, C. A. Ortiz and G. Z. Adunas, hep-ph/0006092; T. Kitabayashi and M. Yasue, hep-ph/0006040. M. Matsuda, C. Jarlskog, S. Skadhauge and

M. Tanimoto, hep-ph/0005147; A. Ghosal, Phys. Rev. D **62**, 092001 (2000); Q. Shafi and Z. Tavartkiladze, Phys. Lett. B **482**, 145 (2000); R. N. Mohapatra, A. Perez-Lorenzana and C. A. de Sousa Pires, Phys. Lett. B **474**, 355 (2000); Q. Shafi and Z. Tavartkiladze, Phys. Lett. B **487**, 145 (2000); Z. Xing, Phys. Rev. D **61**, 057301 (2000); C. S. Kim and J. D. Kim, Phys. Rev. D **61**, 057302 (2000); C. H. Albright and S. M. Barr, Phys. Lett. B **461**, 218 (1999); H. B. Benaoum and S. Nasri, Phys. Rev. D **60**, 113003 (1999); A. Ghosal, hep-ph/9905470; M. Jezabek and Y. Sumino, Phys. Lett. B **457**, 139 (1999); C. Jarlskog, M. Matsuda, S. Skadhauge and M. Tanimoto, Phys. Lett. B **449**, 240 (1999); R. N. Mohapatra and S. Nussinov, Phys. Rev. D **60**, 013002 (1999); R. N. Mohapatra and S. Nussinov, Phys. Lett. B **441**, 299 (1998); S. Davidson and S. F. King, Phys. Lett. B **445**, 191 (1998);

[12] N. Haba, Phys. Rev. **D59**, 035011 (1998).

[13] H. Georgi and C. Jarlskog, Phys. Lett. B **86**, 297 (1979).

[14] V. Barger, M.S. Berger, P. Ohmann, Phys. Rev. D **47**, 1093 (1993).

[15] D. E. Groom *et al.* [Particle Data Group Collaboration], Eur. Phys. J. C **15**, 1 (2000).

[16] K.S. Babu, C.N. Leung, J. Pantaleone, Phys. Lett. B **319**, 191 (1993).

[17] T. Toshito [SuperKamiokande Collaboration], hep-ex/0105023.

[18] S. F. King, hep-ph/0105261.

[19] G. Eyal, Phys. Lett. B **441**, 191 (1998) [hep-ph/9807308].

[20] R. Barbieri, L. Giusti, L. J. Hall and A. Romanino, Nucl. Phys. B **550**, 32 (1999) [hep-ph/9812239].

[21] R. G. Roberts, A. Romanino, G. G. Ross and L. Velasco-Sevilla, hep-ph/0104088; T. Blazek, S. Raby and K. Tobe, Phys. Rev. D **62** (2000) 055001;

[22] T. Banks and M. Dine, Phys. Rev. D **45**, 1424 (1992);

[23] M. Green and J. Schwarz, Phys. Lett. B **149**, 117 (1984).

[24] R. Dermisek and S. Raby, Phys. Rev. D **62**, 015007 (2000) [hep-ph/9911275].